EFFECT OF A CONDUCTING SCREEN ON THE STATE OF POLARIZATION OF THE WAVE DIFFRACTED ON A SEMI-PLANE

By A. Domański

Institute of Physics, Technical University, Warsaw*

(Received Apil 1, 1971)

States of polarization of the wave diffracted on a semi-plane of finite conductance are analyzed resorting to Wolf's coherence matrix. A discussion is given of the influence of the material constituting the screen, for various polarizations of the incident wave.

1. Introduction

The aim of this paper is to give an analysis of the states of polarization of the wave diffracted on a semi-plane of finite conductivity, in the zone of shadow and at a large distance from the diffracting edge, resorting to Wolf's coherence matrix. We start from the modified Sommerfeld solution due to Raman and Krishnan [1]. It will be remembered [2] that it was Sommerfeld who solved the diffraction problem for a perfectly conducting semi-plane. His solutions of the wave equation in cylindrical coordinates (Fig. 1) were:

$$u = F(\varrho, \Phi, \Phi_0) - F(\varrho, \Phi, -\Phi_0) \tag{1.1a}$$

$$u = F(\varrho, \Phi, \Phi_0) + F(\varrho, \Phi, -\Phi_0) \tag{1.1b}$$

respectively for the electric component (1.1a), for parallel planes of polarization and incidence, for the magnetic component (1.1b) at perpendicular configuration of the planes. The functions $F(\varrho, \Phi, \Phi_0)$ and $F(\varrho, \Phi, -\Phi_0)$ are defined as follows:

$$F(\varrho, \Phi, \Phi_0) = \left(\frac{i}{\pi}\right)^{1/2} e^{i\omega t} e^{ik\varrho\cos(\Phi-\Phi_0)} \int_{-\infty}^{\tau} e^{-i\lambda^2} d\lambda \tag{1.2a}$$

where $\tau = (2\pi\varrho)^{1/2} \cos\frac{1}{2}(\Phi-\Phi_0)$,
and

$$F(\varrho, \Phi, -\Phi_0) = \left(\frac{i}{\pi}\right)^{1/2} e^{i\omega t} e^{ik\varrho\cos(\Phi+\Phi_0)} \int_{-\infty}^{\tau} e^{-i\lambda^2} d\lambda \tag{1.2b}$$

where $\tau = (2\pi\varrho)^{1/2} \cos\frac{1}{2}(\Phi+\Phi_0)$.

* Address: Instytut Fizyki, Politechnika Warszawska, Warszawa, Koszykowa 75, Poland.

Finally, Sommerfeld's solutions for the diffracted wave, in the shadow zone at large ϱ-values, are of the form:

$$E_z = -\frac{e^{-i(k\varrho-\omega t+\pi/4)}}{2(2\pi k\varrho)^{1/2}}\left[\frac{1}{\cos\frac{1}{2}(\Phi-\Phi_0)}-\frac{1}{\cos\frac{1}{2}(\Phi+\Phi_0)}\right], \tag{1.3a}$$

$$H_z = -\frac{e^{-i(k\varrho-\omega t+\pi/4)}}{2(2\pi k\varrho)^{1/2}}\left[\frac{1}{\cos\frac{1}{2}(\Phi-\Phi_0)}+\frac{1}{\cos\frac{1}{2}(\Phi+\Phi_0)}\right]. \tag{1.3b}$$

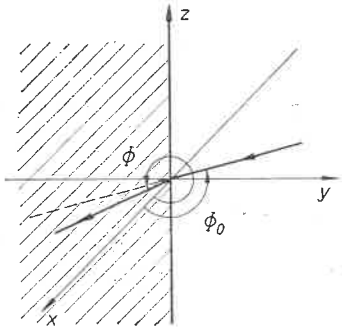

Fig. 1. Definition of: angle on incidence Φ_0, angle of diffraction Φ, plane of incidence $0xy$, and diffracting edge $0z$

Raman and Krishnan [1] introduced coefficients C_s+iD_s and C_p+iD_p, adjusted to represent the amplitude of the wave reflected at the illuminated side of the screen, for some well-defined angle. They postulate solutions of the form:

$$u = F(\varrho, \Phi, \Phi_0)-(C_s+iD_s)F(\varrho, \Phi, -\Phi_0) \tag{1.4a}$$

$$u = F(\varrho, \Phi, \Phi_0)+(C_p+iD_p)F(\varrho, \Phi, -\Phi_0) \tag{1.4b}$$

where the functions $F(\varrho, \Phi, \Phi_0)$ and $F(\varrho, \Phi, -\Phi_0)$ are similar to those of Sommerfeld (1.2).

In the zone of shadow and at large values of ϱ, the functions for the wave diffracted at the edge of a screen of the above-defined kind are:

$$E_z = -\frac{e^{-i(k\varrho-\omega t+\pi/4)}}{2(2\pi k\varrho)^{1/2}}\left[\frac{1}{\cos\frac{1}{2}(\Phi-\Phi_0)}-\frac{C_s+iD_s}{\cos\frac{1}{2}(\Phi+\Phi_0)}\right] \tag{1.5a}$$

$$H_z = -\frac{e^{-i(k\varrho-\omega t+\pi/4)}}{2(2\pi k\varrho)^{1/2}}\left[\frac{1}{\cos\frac{1}{2}(\Phi-\Phi_0)}+\frac{C_p+iD_p}{\cos\frac{1}{2}(\Phi+\Phi_0)}\right]. \tag{1.5b}$$

The analysis of the states of polarization of the diffracted wave in the zone of shadow was performed for large values of ϱ, since Wolf's coherence matrix [3] is applicable to plane or locally plane waves only, and this condition is fulfilled by diffracted waves only in the far zone. Since the problem is symmetric with respect to the edge of the screen insofar as regards the solutions of Raman and Krishnan, the present considerations are restricted to the case when the wave vector is perpendicular to the edge. The considerations are for a monochromatic wave, but can be extended to that of a quasi-monochromatic one [4].

An analysis of the states of polarization of the diffracted wave, using Wolf's coherence matrix, is due to Karczewski and Wolf [5] for screens fulfilling conditions of the "Kirchhoff type" of approximate electric theory and approximate magnetic theory with arbitrarily shaped aperture, and to Jannson [4] for the perfectly conducting semi-plane.

2. *Coherence matrix for the incident and diffracted wave*

The polarization of a plane electromagnetic wave is fully defined by its propagation direction, as represented by the versor $\vec{n}$ of its wave vector $\vec{k}$, and the components of its electric vector $\vec{E}$ or magnetic vector $\vec{H}$. This is so because, for a plane wave, we have the relations:

$$\vec{H} = \vec{n} \times \vec{E}, \; \vec{n} \cdot \vec{E} = 0. \tag{2.1}$$

We shall thus consider henceforth the components of $\vec{E}$ only.

We construct the coherence matrix for the components of $\vec{E}$ parallel and perpendicular to the edge of the screen, since the conditions of diffraction are known for these components. We accordingly introduce a supplementary coordinate system with axes L, M, K such

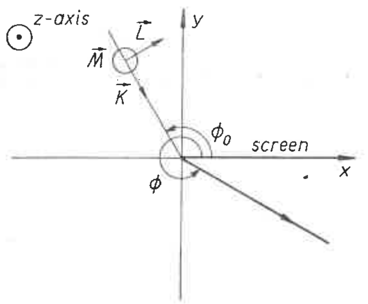

Fig. 2. Orientation of versors $\vec{K}$, $\vec{L}$, $\vec{M}$

that the component E_L shall represent the electric vector of a plane wave with polarization perpendicular to the edge of the screen, whereas the component E_M shall represent parallel polarization (Fig. 2).

With regard to Fig. 2, we have the relations:

$$\vec{L} \times \vec{M} = \vec{K}, \vec{L} \cdot \vec{K} = 0. \tag{2.2}$$

Assume

$$E_L(t) = E_{L0} e^{-i(k\varrho - \omega t)}, \; E_M(t) = E_{M0} e^{-i(k\varrho - \omega t)}, \tag{2.3}$$

with E_{L0} and E_{M0} given by:

$$E_{L0} = a_L e^{i\Psi_L}, \; E_{M0} = a_M e^{i\Psi_M}. \tag{2.4}$$

With the preceding notations, the coherence matrix of the incident wave is of the form:

$$I_0 = \begin{bmatrix} \langle E_L E_L^* \rangle, & \langle E_L E_M^* \rangle \\ \langle E_L^* E_M \rangle, & \langle E_M E_M^* \rangle \end{bmatrix} = \begin{bmatrix} a_L^2, & a_L a_M e^{i(\Psi_L - \Psi_M)} \\ a_L a_M e^{-i(\Psi_L - \Psi_M)}, & a_M^2 \end{bmatrix}. \tag{2.5}$$

The diffracted wave component parallel to the edge is given by (1.5a), whereas the perpendicular component is to be had from the relation

$$E_{\perp} = H_z \tag{2.6}$$

with H_z given by Eq. (1.5b).

Introducing now coordinates l, m, p as shown in Fig. 3, we obtain:

$$\vec{l} \times \vec{m} = \vec{p}, \quad \vec{l} \cdot \vec{p} = 0. \tag{2.7}$$

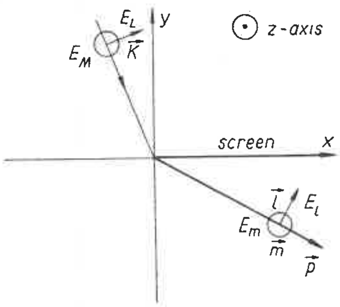

Fig. 3. Orientation of versors $\vec{l}$, $\vec{m}$, $\vec{p}$

In coordinates l, m, p, taking into consideration phase, and assuming the incident amplitudes in the form E_{L0} and E_{M0}, we obtain:

$$E_l = A_1 E_{L0} e^{-i(k\varrho - \omega t + \pi/4)}, \quad E_m = A_2 E_{M0} e^{-i(k\varrho - \omega t + \pi/4)} \tag{2.8}$$

where

$$A_1 = -\frac{1}{2(2\pi k\gamma)^{1/2}} \left[\frac{1}{\cos\frac{1}{2}(\Phi - \Phi_0)^{1/2}} + \frac{C_p + iD_p}{\cos\frac{1}{2}(\Phi + \Phi_0)} \right] = r_1 e^{i\varphi_1}, \tag{2.9a}$$

$$A_2 = -\frac{1}{2(2\pi k\varrho)^{1/2}} \left[\frac{1}{\cos\frac{1}{2}(\Phi - \Phi_0)} - \frac{C_s + iD_s}{\cos\frac{1}{2}(\Phi + \Phi_0)} \right] = r_2 e^{i\varphi_2}. \tag{2.9b}$$

The coherence matrix for the diffracted wave takes the form:

$$I = \begin{bmatrix} \langle E_l E_l^* \rangle, \langle E_l E_m^* \rangle \\ \langle E_l^* E_m \rangle, \langle E_m E_m^* \rangle \end{bmatrix} = \begin{bmatrix} A_1 A_1^* \langle E_L E_L^* \rangle, A_1 A_2^* \langle E_L E_M^* \rangle \\ A_1^* A_2 \langle E_L^* E_M \rangle, A_2 A_2^* \langle E_M E_M^* \rangle \end{bmatrix}.$$

$$= \begin{bmatrix} A_1 A_1^* I_{LL}, A_1 A_2^* I_{LM} \\ A_1^* A_2 I_{ML}, A_2 A_2^* I_{MM} \end{bmatrix} = \begin{bmatrix} I_{ll}, I_{lm} \\ I_{ml}, I_{mm} \end{bmatrix} \tag{2.10}$$

with $I_{LL}, I_{LM}, I_{ll}, I_{lm}$ — the coherence matrix elements for the incident and diffracted waves, respectively.

3. *Analysis of the states of polarization of the diffracted wave*

By Eq. (2.10) it results that if the incident wave is totally polarized ($\det I_0 = 0$), the diffracted wave is totally polarized, too ($\det I = 0$). As a matter of fact, we have:

$$\det I = |A_1|^2 |A_2|^2 \det I_0. \tag{3.1}$$

By (2.5), the coherence matrix for the case when the incident wave is linearly polarized can be written in the form:

$$I_0^l = \begin{bmatrix} a_L^2, & a_L a_M e^{in\pi} \\ a_L a_M e^{-in\pi}, & a_M^2 \end{bmatrix} \tag{3.2}$$

where $n = 0, \pm 1, \pm 2, \ldots$

By (2.10), the coherence matrix for the diffracted wave is:

$$I^l = \begin{bmatrix} |A_1|^2 a_L^2, & A_1 A_2^* a_L a_M e^{in\pi} \\ A_1^* A_2 a_L a_M e^{-in\pi}, & |A_2|^2 a_M^2 \end{bmatrix}$$

$$= \begin{bmatrix} r_1^2 a_L^2, & r_1 r_2 a_L a_M e^{i(\varphi_1 - \varphi_2 + n\pi)} \\ r_1 r_2 a_L a_M e^{-i(\varphi_1 - \varphi_2 + n\pi)}, & r_2^2 a_M^2 \end{bmatrix}. \tag{3.3}$$

The diffracted wave is now elliptically polarized, and can be described by the ratio of axes and the angle of inclination of the larger axis with respect to the coordinate axes l, m, p. Denoting the angle between the larger axis of the ellipse and the l-axis by Ω, we have by Ref. [6]:

$$\operatorname{tg} 2\Omega = \frac{I_{lm} + I_{ml}}{I_{ll} - I_{mm}}$$

$$= \frac{r_1 r_2 a_L a_M [e^{i(\varphi_1 - \varphi_2 + n\pi)} + e^{-i(\varphi_1 - \varphi_2 + n\pi)}]}{r_1^2 a_L^2 - r_2^2 a_M^2} = \frac{2 r_1 r_2 a_L a_M \cos(\varphi_1 - \varphi_2 + n\pi)}{r_1^2 a_L^2 - r_2^2 a_M^2}, \tag{3.4}$$

whereas the ratio of axes of the ellipse is now:

$$s = \frac{i(I_{lm} - I_{ml})}{I_{ll} + I_{mm}} = -\frac{2 r_1 r_2 a_L a_M \sin(\varphi_1 - \varphi_2 + n\pi)}{r_1^2 a_L^2 + r_2^2 a_M^2}. \tag{3.5}$$

If the incident wave is circularly polarized, its coherence matrix is of the form:

$$I_0^c = \begin{bmatrix} a_L^2, & a_L a_M e^{in\pi/2} \\ a_L a_M e^{-in\pi/2}, & a_M^2 \end{bmatrix} = \begin{bmatrix} a^2, & a^2 e^{in\pi/2} \\ a^2 e^{-in\pi/2}, & a^2 \end{bmatrix} \tag{3.6}$$

with $a = a_L = a_M$ and $n = \pm 1, \pm 3, \ldots$

In this case, the coherence matrix of the diffracted wave is:

$$I^c = \begin{bmatrix} |A_1|^2 a^2, & A_1 A_2^* a^2 e^{in\pi/2} \\ A_1^* A_2 a^2 e^{-in\pi/2}, & |A_2|^2 a^2 \end{bmatrix} = \begin{bmatrix} r_1^2 a^2, & r_1 r_2 a^2 e^{i(\varphi_1 - \varphi_2 + n\pi/2)} \\ r_1 r_2 a^2 e^{-i(\varphi_1 - \varphi_2 + n\pi/2)}, & r_2^2 a^2 \end{bmatrix}. \tag{3.7}$$

The diffracted wave is elliptically polarized; the inclination of the large axis with respect to the l-axis is now:

$$\operatorname{tg} 2\Omega = \frac{I_{lm}+I_{ml}}{I_{ll}-I_{mm}} = \frac{2r_1r_2 \cos(\varphi_1-\varphi_2+n\pi/2)}{r_1^2-r_2^2} \tag{3.8}$$

and the ratio of axes takes the form:

$$s = \frac{i(I_{lm}-I_{ml})}{I_{ll}+I_{mm}} = -\frac{2r_1r_2 \sin(\varphi_1-\varphi_2+n\pi/2)}{r_1^2+r_2^2}. \tag{3.9}$$

If the incident wave is elliptically polarized, its coherence matrix is of the form:

$$I_0^e = \begin{bmatrix} a_L^2, & a_La_Me^{i(\Psi_L-\Psi_M)} \\ a_La_Me^{-i(\Psi_L-\Psi_M)}, & a_M^2 \end{bmatrix}. \tag{3.10}$$

That of the diffracted wave is now:

$$I^e = \begin{bmatrix} |A_1|^2a_L^2, & A_1A_2^*a_La_Me^{i(\Psi_L-\Psi_M)} \\ A_1^*A_2a_La_Me^{-i(\Psi_L-\Psi_M)}, & |A_2|^2a_M^2 \end{bmatrix}$$

$$= \begin{bmatrix} r_1^2a_L^2, & r_1r_2a_La_Me^{i(\varphi_1-\varphi_2+\Psi_L-\Psi_M)} \\ r_1r_2a_La_Me^{-i(\varphi_1-\varphi_2+\Psi_L-\Psi_M)}, & r_2^2a_M^2 \end{bmatrix}. \tag{3.11}$$

The diffracted wave, too, is elliptically polarized. However, the angle (denoted by Ω_0) between the large axis of the ellipse of the incident wave and the plane of incidence can vary; this variability is characterized by means of the factor g of Ref. [6]:

$$g = \frac{\operatorname{tg} 2\Omega}{\operatorname{tg} 2\Omega_0} = \frac{I_{lm}+I_{ml}}{I_{LM}+I_{ML}} \cdot \frac{I_{LL}-I_{MM}}{I_{ll}-I_{mm}}$$

$$= \frac{r_1r_2\,[e^{i(\varphi_1-\varphi_2+\psi_L-\psi_M)}+e^{-i(\varphi_1-\varphi_2+\psi_L-\psi_M)}](a_L^2-a_M^2)}{[e^{i(\psi_L-\psi_M)}+e^{-i(\psi_L-\psi_M)}]\,(r_1^2a_L^2-r_2^2a_M^2)}$$

$$= \frac{\cos(\varphi_1-\varphi_2+\Psi_L-\Psi_M)\cdot r_1r_2(a_L^2-a_M^2)}{\cos(\Psi_L-\Psi_M)\cdot(r_1^2a_L^2-r_2^2a_M^2)}. \tag{3.12}$$

The variability of the ratio of axes can be expressed by way of the factor d of Ref. [6]:

$$d = \frac{I_{lm}-I_{ml}}{I_{LM}-_{ML}} \cdot \frac{I_{LL}+I_{MM}}{I_{ll}+I_{mm}} = \frac{\sin(\varphi_1-\varphi_2+\Psi_L-\Psi_M)}{\sin \Psi_L-\Psi_M)} \cdot \frac{r_1r_2(a_L^2+a_M^2)}{(r_1^2a_L^2+r_2^2a_M^2)}. \tag{3.13}$$

The polarization properties of a partially polarized wave are defined by the polarization ratio P [3] which, for the incident wave, is of the form:

$$P_0 = \frac{I_{0\text{polar}}}{I_{0\text{total}}} = \left[1-\frac{4\det I_0}{(I_{LL}+I_{MM})^2}\right]^{1/2}. \tag{3.14}$$

For the diffracted wave, one has:

$$P = \frac{I_{\text{polar}}}{I_{\text{total}}} = \left[1-\frac{4\det I}{(I_{ll}+I_{mm})^2}\right]^{1/2} = \left[1-\frac{4r_1^2r_2^2\det I_0}{(r_1^2I_{ll}+r_2^2I_{MM})^2}\right]^{1/2}. \tag{3.15}$$

4. *Influence of the material of a conducting screen on the state of polarization of the diffracted wave*

The influence exerted by the properties of the material of which the screen is made resides in its reflection coefficient which, for a given wavelength, takes various values from one metal to another. Assuming for simplicity that the incident wave is perpendicular to the screen ($\Phi_0 = \pi/2$), this coefficient becomes:

$$R = C_s + iD_s = C_p + iD_p = C + iD. \tag{4.1}$$

For a perfect conductor $R = 1$, whereas for gold and steel at $\lambda = 0.58\times 10^{-6}$m the reflection coefficient amounts to $R_{Au} = 0.71 - i0.57$ and $R_{St} = 0.69 - i0.29$ [1] respectively.

In order to simplify our further considerations, we introduce coefficients h_I and $\Delta\varphi$, defined as follows:

$$h_I = \frac{|A_1|}{|A_2|} = \frac{r_1}{r_2} = \left\{ \frac{\left[\cos\frac{1}{2}\left(\Phi + \frac{\pi}{2}\right) + C\cos\frac{1}{2}\left(\Phi - \frac{\pi}{2}\right)\right]^2 + \left[D\cos\frac{1}{2}\left(\Phi - \frac{\pi}{2}\right)\right]^2}{\left[\cos\frac{1}{2}\left(\Phi + \frac{\pi}{2}\right) - C\cos\frac{1}{2}\left(\Phi - \frac{\pi}{2}\right)\right]^2 + \left[D\cos\frac{1}{2}\left(\Phi - \frac{\pi}{2}\right)\right]^2} \right\}^{1/2} \tag{4.2}$$

$$\Delta\varphi = \arg A_1 - \arg A_2 = \varphi_1 - \varphi_2$$

$$= \operatorname{arc\,tg} \frac{D\cos\frac{1}{2}\left(\Phi - \frac{\pi}{2}\right)}{C\cos\frac{1}{2}\left(\Phi - \frac{\pi}{2}\right) + \cos\frac{1}{2}\left(\Phi + \frac{\pi}{2}\right)} - \operatorname{arc\,tg} \frac{D\cos\frac{1}{2}\left(\Phi - \frac{\pi}{2}\right)}{C\cos\frac{1}{2}\left(\Phi - \frac{\pi}{2}\right) - \cos\frac{1}{2}\left(\Phi + \frac{\pi}{2}\right)}. \tag{4.3}$$

The dependence of h_I and $\Delta\varphi$ in function of the angle Φ is plotted in Fig. 4 for the perfect conductor as well as for gold and steel.

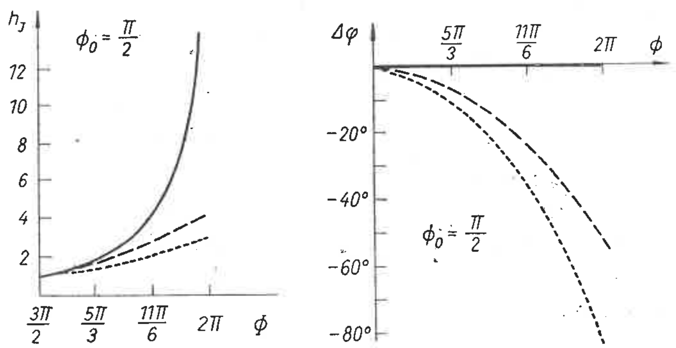

Fig. 4. Graphs of the coefficients h_I and $\Delta\varphi$ *vs.* the diffraction angle Φ, for the perfect conductor (continuous line), steel (dashed line), and gold (dotted line)

In the case of a linearly polarized incident wave the diffracted wave is, as stated in the previous Section, ellip ically polarized; the deviation of the large axis of the ellipse from the l-axis is, expressed in terms of h_I and $\Delta\varphi$,

$$\operatorname{tg} 2\Omega = \frac{2h_I \dfrac{a_L}{a_M} \cos(\Delta\varphi + n\pi)}{h_I^2 \left(\dfrac{a_L}{a_M}\right)^2 - 1}. \tag{4.4}$$

whereas the ratio of axes amounts to:

$$s = -\frac{2h_I \dfrac{a_L}{a_M} \sin(\Delta\varphi + n\pi)}{h_I^2 \left(\dfrac{a_L}{a_M}\right)^2 + 1}. \tag{4.5}$$

Graphs of $\Omega = f(\Phi)$ and $s = f(\Phi)$ for the perfect conductor, gold and steel, are to be found in Fig. 5.

As results from the shape of $s = f(\Phi)$, the diffracted wave is always linearly polarized (this is a degenerate form of elliptical polarization) in the case of the perfect conductor

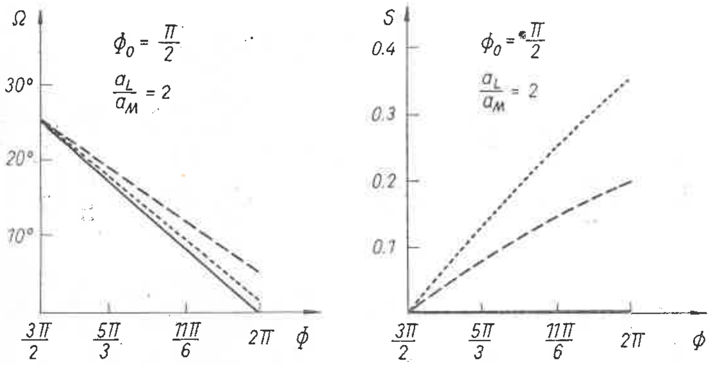

Fig. 5. Graphs of the inclination angle Ω between the large axis of the polarization ellipse and the l-axis, as well as of the ratio of axes s *vs.* the angle of diffraction Φ, for the perfect conductor (continuous line), steel (dashed line) and gold (dotted line) for the case of a linearly polarized incident wave

whereas, for real conductors, the ratio of axes of the polarization ellipse grows in function of the angle Φ. Moreover, in the zone of shadow, the inclination of the large axis with respect to the l-axis decreases in function of the angle Φ in all cases, though somewhat less steeply in those of gold and steel. At the surface of the screen ($\Phi = 2\pi$), the angle of inclination differs from zero for real conductors only, and depends on the material of the screen.

With the incident wave polarized circularly, the diffracted wave is polarized elliptically. The inclination now is:

$$\operatorname{tg} 2\Omega = \frac{2h_I \cos(\Delta\varphi + n\pi/2)}{h_I^2 - 1}. \tag{4.6}$$

From the way this function depends on the angle Φ it results that for the perfect conductor the large axis of the polarization ellipse coincides with the l-axis throughout the entire zone of shadow but exhibits a constant inclination in the case of real conductors amounting to $\Omega_{Au}=11°20'$ for gold and to $\Omega_{St} = 19°25'$ for steel ($\text{tg}\, 2\Omega = -D/C$). The ratio of axes is given here as follows:

$$s = -\frac{2h_I \sin(\Delta\varphi + n\pi/2)}{h_I^2+1}. \tag{4.7}$$

From the graph of $s = f(\Phi)$ (Fig. 6), the ratio of axes varies more slowly in the case of a real conductor than in that of the perfect conductor. Significantly, however, the differences

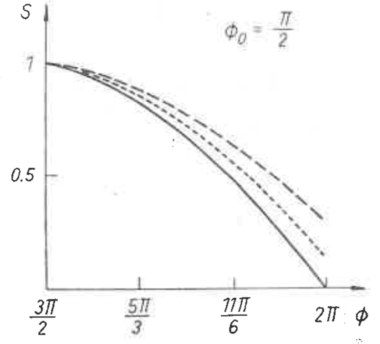

Fig. 6. Ratio s of axes $vs.$ the diffraction angle Φ, for the perfect conductor (continuous line), steel (dashed line), and gold (dotted line), for the case of a circularly polarized incident wave

in this respect are but slight — an essentially important result from the experimental point of view.

With the incident wave elliptically polarized, the diffracted wave is elliptically polarized too. The variation in inclination of the large axis is given by the factor g:

$$g = \frac{\cos(\Delta\varphi + \Delta\Psi)}{\cos \Delta\Psi} \cdot \frac{h_I\left[\left(\frac{a_L}{a_M}\right)^2 - 1\right]}{h_I^2\left(\frac{a_L}{a_M}\right)^2 - 1} \tag{4.8}$$

where $\Delta\Psi = \Psi_L - \Psi_M$. The behaviour of this inclination is shown in Fig. 7 in function of the angle Φ. For the perfect conductor, the angle subtended by the large axis and the l-axis decreases to zero in function of the diffraction angle whereas for real conductors this tendency is weaker so that even at $\Phi = 2\pi$ the large axis fails to coincide with the l-axis. It is significant that the factor g, for real conductors, depends not only on the parameter a_L/a_M of the incident wave but, moreover, on the difference in phase $\Delta\Psi$ of its components. The factor d describing the variation of the ratio of axes depends, too, on the same parameters of the incident wave:

$$d = \frac{\sin(\Delta\varphi + \Delta\Psi)}{\sin \Delta\Psi} \cdot \frac{h_I\left[\left(\frac{a_L}{a_M}\right)^2 + 1\right]}{h_I^2\left(\frac{a_L}{a_M}\right)^2 + 1}. \tag{4.9}$$

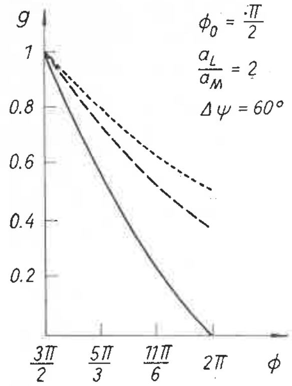

Fig. 7. Inclination of the large axis of the polarization ellipse with respect to the l-axis *vs.* the diffraction angle Φ, for the perfect conductor (continuous line), steel (dashed line), and gold (dotted line), for the case of an elliptically polarized incident wave

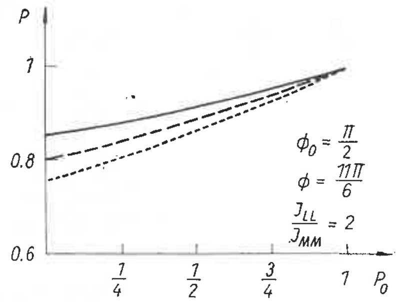

Fig. 8. Polarization ratio P of the diffracted wave *vs.* polarization ratio P_0 of the incident wave, for the perfect conductor (continuous line), steel (dashed line), and gold (dotted line)

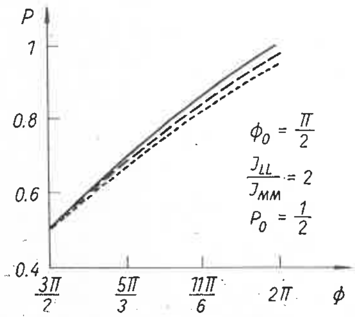

Fig. 9. Polariration ratio P *vs.* the diffraction angle, for the perfect conductor (continuous line), steel (dashed line), and gold (dotted line)

The presence of the factor sin $(\Delta\varphi+\Delta\Psi)$ in Eq. (4.9) suggests that for certain angles Φ, for which $\Delta\varphi=-\Delta\Psi$, the diffracted wave will exhibit linear polarization ($d=0$).

Eqs (3.14) and (3.15) enable us to express the polarization ratio P of the diffracted wave in terms of the ratio P_0 of the incident wave:

$$P=\left[1-(1-P_0^2)h_I^2\left(\frac{\dfrac{I_{LL}}{I_{MM}}+1}{h_I^2\dfrac{I_{LL}}{I_{MM}}+1}\right)^2\right]^{1/2}. \tag{4.10}$$

From the shape of $P=f(P_0)$ as plotted in Fig. 8 for $I_{LL}/I_{MM}>1$, the polarizing properties of the real conductor are seen to be worse than those of the perfect one.

The same conclusion can be drawn from the graph of $P=f(\Phi)$ (Fig. 9). The diffracted wave is more strongly polarized than the incident wave and tends to total polarization ($P=1$) for the case of the real conductor, whereas in that of gold or steel the polarization remains partial even at the surface of the screen. The situation is somewhat different for $I_{LL}/I_{MM}<1$, when $P=f(h_I)$ exhibits a minimum for $h_{I\,\min}=(I_{MM}/I_{LL})^{1/2}$, amounting to $P_{\min}=(I_{LM}I_{ML}/I_{LL}I_{MM})^{1/2}$.

The formalism of the coherence matrix [3] permits a representation of the matrix of a partially polarized wave as the sum of matrices of the totally polarized and totally unpolarized waves. We thus have:

$$I_{LL}=I^p_{LL}+I^n,\quad I_{LM}=I^p_{LM} \tag{4.11}$$
$$I_{ML}=I^p_{ML},\quad I_{MM}=I^p_{MM}+I^n$$

where I^p_{LL}, I^p_{MM}, ... are elements of the coherence matrix of the totally polarized part of the incident wave and I^n is the element of that of the totally unpolarized part. With regard to this, and on inserting the polariation ratio P_0 of the incident wave into the formulas for $h_{I\,\min}$ and $P_{\min}$, we obtain:

$$h_{I\,\min}=\left[\frac{\dfrac{I^p_{LL}}{I^p_{MM}}+\dfrac{1+P_0}{1-P_0}}{1+\dfrac{I^p_{LL}}{I^p_{MM}}\cdot\dfrac{(1+P_0)}{(1-P_0)}}\right]^{1/2}. \tag{4.12a}$$

$$P_{\min}=\left[\frac{4P_0^2\dfrac{I^P_{LL}}{I^P_{MM}}}{(1-P_0^2)\left(1+\dfrac{I^P_{LL}}{I^P_{MM}}\right)^2+4P_0^2\dfrac{I^P_{LL}}{I^P_{MM}}}\right]^{1/2}. \tag{4.12b}$$

If $I^p_{LL}/I^p_{MM}=0$, the diffracted wave can be totally unpolarized; this will occur for various angles Φ according to the kind of screen, since for $I^p_{LL}/I^p_{MM}=0$ one has $h_{I\,\min}=[(1+P_0)/(1-P_0)]^{1/2}$. A similar effect is obtained in approximate electric and magnetic theory [7] as well as in Sommerfeld's exact theory for the perfect conductor [4].

5. *Conclusions*

The introduction by Raman and Krishnan of a reflection coefficient into the Sommerfeld solutions permitted to relate diffraction with the parameters characterizing the material of the diffracting screen. Coherence matrix formalism, applied to these solutions, has paved the way for a study of the states of polarization of the diffracted wave leading essentially to the following conclusions:

a) A screen consisting of a real conductor affects not only the amplitudes but moreover the phases of the components perpendicular and parallel to the diffracting edge; this is not the case for the perfectly conducting screen;

b) With incident wave linearly polarized, the diffracted wave is elliptically polarized, whereas in the case of the perfect conductor it remains linearly polarized always;

c) With the incident wave circularly polarized, the diffracted wave is elliptically polarized, the large axis of the polarization ellipse subtending a constant angle with the l-axis even for the smallest diffraction angles; in the case of the perfect conductor, however, the large axis remains perpendicular to the screen always;

d) With the incident wave elliptically polarized, the diffracted wave can be linearly polarized for some angles.

Conclusions c and d appear to be the easiest for experimental checking.

All the functions describing the states of polarization of the diffracted wave depend in a highly involved manner on the angle of diffraction Φ making it necessary to introduce the coefficients h_l and $\Delta\varphi$; in order to proceed to plotting these functions, the two parameters had first to be determined and assumptions made concerning the parameters of the incident wave.

The author wishes to thank Professor Dr habil. B. Karczewski for his valuable hints and advice. Thanks are also due to T. Jannson, M. Sci., for his numerous discussions relating to some problems of the present paper.

REFERENCES

[1] C. V. Raman, K. S. Krishnan, *Proc. Roy. Soc.*, (A), **116**, London 1927.
[2] B. Baker, E. Copson, *Mathematical Theory of Huygens Principle*, Pergamon Press, Edynburg 1939.
[3] M. Born, E. Wolf, *Principles of Optics*, Pergamon Press, New York 1965.
[4] T. Jannson, *Acta Phys. Polon.*, **36**, 803 (1969).
[5] B. Karczewski, E. Wolf. *J. Opt. Soc. Amer.*, **56**, 1207 (1966).
[6] E. Wolf, *Nuovo Cimento*, **13**, 1180 (1959).
[7] A. Żardecki, *J. Opt. Soc. Amer.* **56**, 1722 (1966).